European Review for Medical and Pharmacological Sciences 2017; 21: 3360-3369

MicroRNA-613 attenuates the proliferation, migration and invasion of Wilms' tumor via targeting FRS2

H.-F. WANG[1], Y.-Y. ZHANG[2], H.-W. ZHUANG[1], M. XU[1]

[1]Department of Pediatric Surgery, Linyi Central Hospital, Linyi, China
[2]Department of Hand and Foot Surgery, Linyi Central Hospital, Linyi, C

Haifeng Wang and Yingying Zhang contributed equally

Abstract. – OBJECTIVE: Wilms' tumor is the most common malignant tumor in children worldwide. Considering the poor therapeutic effect on Wilms' tumor, we determined the effects of microRNA-613 on cell proliferation and metastasis in vitro, providing therapeutic targets for the treatment of Wilms' tumor.

PATIENTS AND METHODS: Quantitative real-time PCR (qRT-PCR) was employed to id the expression level of miR-613. CCK8 a ny formation assays were incorporated to ss cell viability and proliferation capacity. Ce gration and invasion assays were performe investigate the metastasis capacity of Wilms' mor cells. Flow cytometry was u detect ce cycle distribution and cell apo tein lev els were assessed by weste otting ay. The target gene was predicte verifi bioinformatics analysis and l se as

RESULTS: The ex es f i-613 wa downregulated in Wi tumo s compared with adjacent norm ssues (n= erexpression of miR-613 ttenuate Wil or cell viability, prolif sion, and mig tion capacity, as wel nduc ycle arrest at the G0/G1 phase. RS2 was cho the target of miR-613 by bi rmatics analy d a luciferase reporte ay. MiR-613 expres n was inversely corre with S2 in Wilms' tumor tissues. Mor r, rest on of FRS2 rescued the tumor sup ve of miR in Wilms' tumor cell growth astasi

ONCL S: M 13 had a tumor-suppres- fect o umor progression and metas via targe FRS2 *in vitro*, which provided an i ative and candidate target for the diagnosis of Wilms' tumor.

KWords
oRNAs, Proliferation, Metastasis, FRS2, Wilms' tu

Introd on

Wilms' tumor so known as a renal embryonal or, is a mixed bryonal tumor[1]. Wilms' tumor most comm alignant tumor in children and c s a larg ority of the diseases in pediatric surg for approximately 8% of all solid tumors in children[2]. The incidence rate is approximately 2/100 million, the age of onset is 1-3 years old, ak incidence is 3 years old[2]. Combined erap of surgery, chemotherapy, and radiotherapy have greatly improved the prognosis of Wilms' tumor[3]. However, these methods are not only toxic but also have the potential to cause serious adverse reactions. Despite the fact that current domestic and foreign researchs have found some Wilms' tumor related genes, such as WT1, WT2, WTX, CTNNB1 and P53[4-6], the molecular mechanism of Wilms' tumor development remains unclear. Therefore, further exploring the biological characteristics and pathogenesis of Wilms' tumor is of great clinical value to find new therapeutic methods and to improve the survival rate of pediatric patients.

As a type of small non-coding RNA transcript, microRNA is an endogenous RNA of approximately 18 to 25 nucleotides in length[7]. It suppresses gene expression through post-transcriptional regulation in various biological processes[8]. A miRNA can bind to the 3'UTR of its target genes to suppress protein translation[9]. An increasing number of investigations have discovered that miRNAs can play an important role in various cell processes[10]. Therefore, a thorough study of miRNAs may be valuable in explaining the occurrence and development of tumors.

MiR-613, a tumor-related miRNA, is downregulated and plays an anti-oncogene role in several

Corresponding Author: Haifeng Wang, MD; e-mail: scorpiosurgeon@163.com

types of cancers, such as prostate cancer[11], breast cancer[12], osteosarcoma[13] and colorectal cancer[14]. Meanwhile, another work[15] reported that a miRNA participates in the process of Wilms' tumor tumorigenesis. However, the role and mechanism of miR-613 in the progression and development of Wilms' tumor remains unknown.

Patients and Methods

Clinical Samples

The 32 pairs of Wilms' tumor tissues and normal matched control kidney tissues used in our work were obtained from patients undergoing routine surgery at Linyi Central Hospital from 2015-2017. All surgical specimens were collected and then frozen immediately in liquid nitrogen until use. The tumor tissues were diagnosed and confirmed by pathological examination. This research was approved by the Ethics Committee of Shandong University. Written informed consent was signed by all participants (or patients' parents on behalf of the children) before the study.

Cell Lines and Transfection

SK-NEP-1 and G401, human kidney (Wilms' Tumor) cell lines, were purchased from Shanghai Model Cell Bank (Shanghai, China). SK-NEP-1 and G401 cells were cultured in Dulbecco's Modified Eagle Medium (DMEM) supplemented with 10% fetal bovine serum (FBS), 100 U/mL penicillin and 100 μg/mL streptomycin. All cells were cultured in an incubator at 37°C with

MiR-613 mimics and the corresponding negative control (miR-NC), miR-613 inhibitor and its corresponding negative control (inhibitor-NC) were obtained from GenePharma (Guangzhou, China). The FRS2-coding sequence was inserted into the pCDNA3.1 vector (Invitrogen, Carlsbad, CA, USA) for FRS2 overexpression and was confirmed by sequencing. Meanwhile, the knockdown of FRS2 was achieved by siRNA-FRS2. Transfections were performed using Lipofectamine 3000 (Invitrogen, Carlsbad, CA, USA) according to the manufacturer's protocols.

RNA Extraction and qRT-PCR

Total RNA was extracted from collected frozen Wilms' tissues and normal matched control kidney tissues using TRIzol reagent (Invitrogen, Carlsbad, CA, USA) following the manufacturer's protocols. PrimeScript® RT reagent kit (TaKaRa, Dalian, China) was used to synthesize cDNAs. U6 was used for normalization. Then, we performed PCR reactions using the following primers: FRS2, forward, 5'-GTG AGT GCG TTT CC[illegible] and reverse, 5'-TGA GTG GCA A[illegible]AAG GAA CAT T-3'; and U6, forward, 5'-[illegible]CCT TAG GCT GAA CA-3' and reverse, 5'-[illegible]TA TGC CGA GCT CTT GT-3'. The [illegible]RNA level of FRS2 was measured by SYBR Green real-time PCR and normalized to GAPDH using the following primers: FRS2, forward, 5'-GT[illegible]CG CA[illegible]TT TAC CCT CA-3' and reverse, 5'-[illegible]C[illegible]TA A[illegible]TCT GGC TGC-3'; and GAPDH, forward, 5'-[illegible]ard, 5'-[illegible]G AGT TGT TCG TAT[illegible]G G-3' and reverse, 5'-[illegible]AC ATG ATG TGG A[illegible]GCA TT-3'. qPCR was performed using a 7500 Fast Real-Time PCR system (Applied Biosystems, Foster City, CA, USA).

Cell Counting Kit-8 Assay and Colony Formation Assay

Cell viability was detected by a Cell Counting Kit-8 (CCK-8) assay (Promega, Madison, WI, USA) after transfection according to the manufacturer's protocol. The transfected cells were grown in 96-well plates (2000 cells/well), then 10 μL of CCK8 solution was added to 90 μL of DMEM medium and incubated for 3 h, and the absorbance was measured at 450 nm. The absorbance was measured at 12 h, 24 h, 48 h and 72 h after cell transfection.

To further investigate the cell proliferation capacity of Wilms' tumor cells, cells were plated in 6-well plates at a density of 5×10^2 cells per well and cultured for 2 weeks. The colonies were fixed in 70% ice-cold methanol for 10 min, stained with 0.5% crystal violet for another 10 minutes and, then, washed 3 times with phosphate buffered saline (PBS).

Cell Cycle Analysis

For cell cycle analysis, SK-NEP-1 and G401 cells were prepared and stained with propidium iodide (PI) using the BD CycletestPlus DNA Reagent Kit (BD Biosciences, Franklin Lakes, NJ, USA). The relative ratio of cells in the G0/G1, S, or G2/M phase was analyzed by Flowjo 7.6. Each experiment was performed three times.

Cell Apoptosis Analysis

SK-NEP-1 and G401 cell suspensions were prepared and double-stained with 5 μL of Annexin V-FITC and 1 μL of PI 50 μg/mL). After incubating in the dark for 15 min, cells were quantified by a flow cytometer equipped with CellQuest software (BD Bioscience, Franklin Lakes, NJ, USA). The percentage of early apoptotic cells was analyzed by Flowjo7.6. Each experiment was performed three times.

Cell Migration Assay

A wound-healing assay was used to assess the cell migration capacity. Transfected cells were cultured in 6-well plates marked with a horizontal line on the back. The cell layer was scratched with a pipette tip across the confluent cell layer. Then, the cells were washed gently and cultured with serum-free medium for 24-48 h. Wound closure was recorded using a light microscope (DFC500, Leica, Wetzlar, Germany).

Cell Invasion Assay

A transwell assay was performed to measure cell invasion. Cells were cultured in the upper invasion chamber (BD Bioscience, Franklin Lakes, NJ, USA) coated with Matrigel. Serum-free medium was added into the upper chamber, whereas 10% FBS-supplemented medium was added into the lower chamber. After 48 h, the cells cultured on the upper side of the filter, which did not invade through the chamber, were removed. Then, the cells in the lower chamber were fixed using 100% pre-cooled methanol, stained with 0.05% crystal violet and analyzed with a microscope (Olympus, Tokyo, Japan). The values of invading cell[s] were measured by counting five fields per me[mbrane].

Bioinformatics Analysis

Target Scan (http://www.targetscan.[org]/vert_71/) and Star Base v2.0 (http://starbase.sysu.edu.cn/index.php) were utilized to predict the target genes. As shown in the da[tabase], FRS2 was the candidate gene that we ch[ose]. The re[sult] of the bioinformatics analysis [indicate]d th[at] of FRS2 binds to miR-613. [Q]RT-PCR was performed to dete[rmine whether] FRS2 is inversely correlated with miR-613 expressi[on] in Wilms' tumor cells.

Luciferase Reporter A[ssay]

We p[urch]ased the FRS2-3'UTR vector with luciferase reporter from Gene[Chem] (Shanghai, China). Cells were co-transfected with the pGL3 luciferase reporter construct containing the 3′UTR of FRS2 and pRL-TK Renilla luciferase vector (Promega, Shanghai, China) and miR-613 mimics or miR-NC (RiboBio, Guangzhou, China). The Dual-Luciferase assay kit (Promega, Shanghai, China) was used to detect the luciferase signal following manufacturer's instructions. Meanwhile, we mutated the predicted miR-613binding site in the 3'UTR of FRS2 and examined whether this mutation could abrogate the decrease in luciferase activity by miR-613 mimics.

Western Blot Analysis

To investigate the relative protein level, cells were washed with ice-cold PBS and lysed using lysis buffer. Then we measured the concentration of the collected protein using a protein assay kit purchased from Beyotime (Shanghai, China). The extracted protein (20 μg) was denatured and boiled on ice. Sodium dodecyl SDS-PAGE was used to separate the proteins, which were then transferred to polyvinylidene difluoride (PVDF) membranes (Millipore, Billerica, MA, USA). Non-fat milk (5%) was used to block non-specific protein interaction in TBST buffer, which contains Tris-HCl (20 mM), NaCl (150 mM) and Tween 20 (0.05%) at 4°C for 1h. The membranes with proteins bound were incubated overnight at 4°C with fat-free milk with a primary antibody against FRS2 (Absci, Nanjing, China). TBST buffer was used to wash the unbound antibody (10 min each for three washes). Then, the membranes were incubated with secondary antibody conjugated with horseradish peroxidase (1 h) at room temperature. After washing the membranes three times in TBST buffer, we developed the membranes using enhanced chemiluminescence (ECL) (Millipore, Billerica, MA, USA) following the manufacturer's instructions.

Statistical Analysis

SPSS 19.0 software (IBM, Armonk, NY, USA) was used for statistical analysis. Statistical data were presented with Graph-PAD prism software. Quantitative data were presented as the mean ± SD. The independent samples *t*-test (SPSS, USA) was used to perform statistical analysis. The regression and correlation analyses were analyzed using Spearman's chi-squared test. The relative expression of mRNA was measured using the $2^{-\Delta\Delta CT}$. The results were determined to be statistically significant at $p<0.05$.

Results

MiR-613 Expression was Decreased in Wilms' Tumor Tissues

The miR-613 expression level was detected by qRT-PCR in 32 pairs of Wilms' tumor tissues, and normal matched control kidney tissues. The result indicated that miR-613 expression was remarkably decreased in Wilms' tumor tissues compared with the paired normal kidney tissues at the mRNA level (Figure 1A). This evidence implied that miR-613 might play a potential role in Wilms' tumor development and progression.

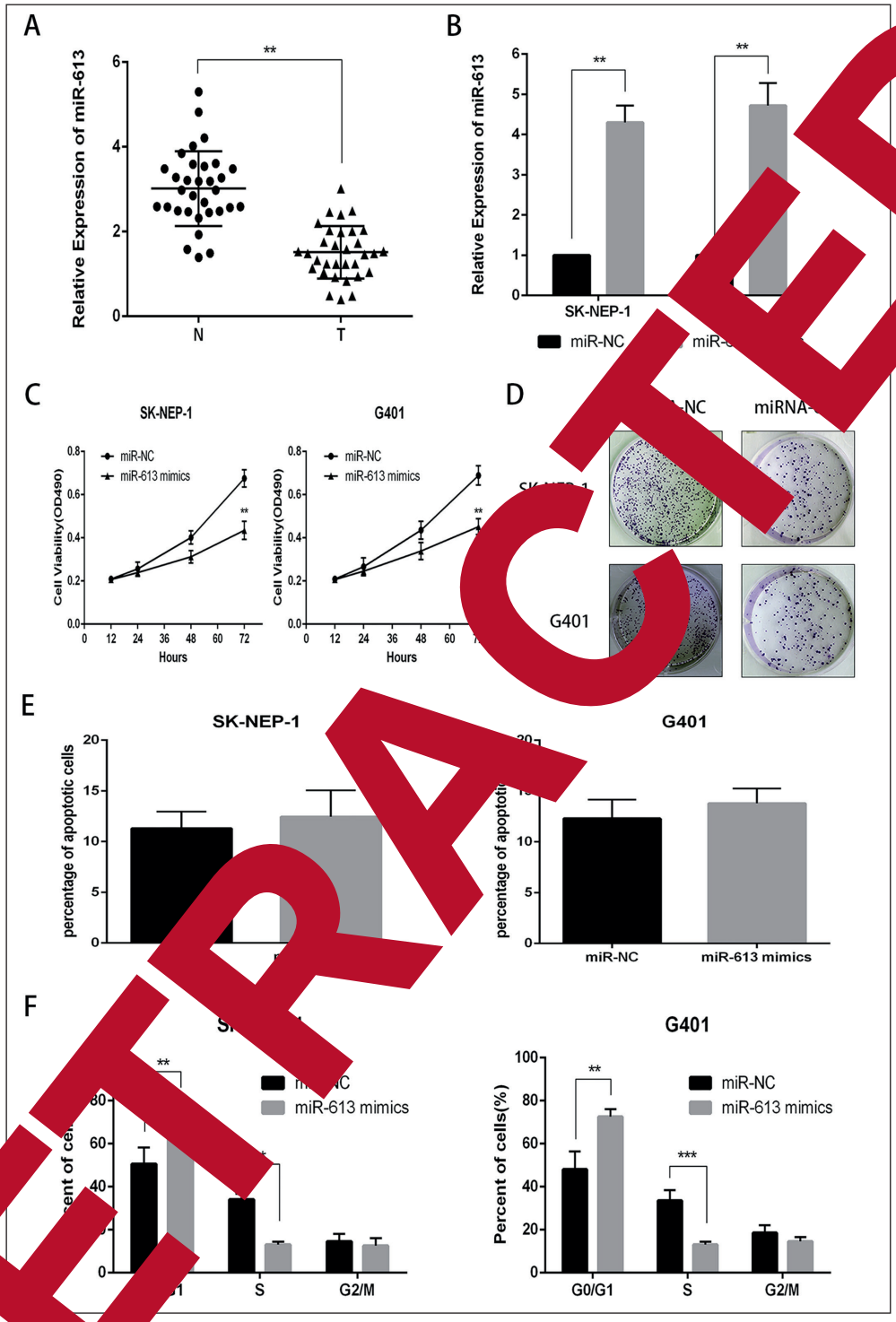

Figure 4. MiR-613 is downregulated in Wilms' tumor tissues and inhibited cell viability and proliferation *in vitro*. **A**, MiR-613 expression level in Wilms' tumor tissues (T) and normal matched control kidney tissues (N), n=32; **B**, Transfection efficiency in SK-NEP-1 and G401 cells transfected with miR-613 mimics and miR-NC; **C**, CCK8 assay was performed to determine the viability of SK-NEP-1 and G401 cells transfected with miR-613 mimics and miR-NC; **D**, Colony formation assay was performed to determine the proliferation of SK-NEP-1 and G401 cells transfected with miR-613 mimics and miR-NC; **E**, Flow cytometric analysis was performed to detect the apoptotic rates of SK-NEP-1 and G401 cells transfected with miR-613 mimics and miR-NC, the results show no difference; **F**, Flow cytometric analysis was performed to detect the cell cycle distribution of SK-NEP-1 and G401 cells transfected with miR-613 mimics and miR-NC. Total RNA was detected by qRT-PCR, and GAPDH was used as an internal control. Data are presented as the mean ± SD of three independent experiments. $^{**}p < 0.01$, $^{***}p < 0.001$.

MiR-613 Inhibited Cell Viability and Proliferation in vitro

To evaluate the biological role of miR-613 in Wilms' tumor tumorigenesis *in vitro*, SK-NEP-1 and G401 cells were transfected with miR-613 mimics and miR-NC to overexpress miR-613 (Figure 1B). Then, we measured cell viability and proliferation using a CCK8 assay in Wilms' tumor cell lines. The viability and proliferation of Wilms' tumor cells were significantly inhibited in a time-dependent manner after transfection with miR-613 mimic compared with miR-NC (Figure 1C).

Meanwhile, we outperformed a colony formation assay to further explore the cell proliferation capacity. The results showed that fewer formed colonies in Wilms' tumor cells transfected with miR-613 mimics compared with miR-NC cells (Figure 1D). Collectively, these results demonstrated that miR-613 can inhibit Wilms' tumor proliferation and viability.

MiR-613 Induced Cell-Cycle Arrest at the G0/G1 Phase

Because miR-613 can regulate the cell proliferation capacity, we determined whether apo[illegible]is and the cell cycle were also affected by [illegible]. As shown by flow cytometric analysis, the [illegible]as no influence of miR-613 on Wilms' tumo[illegible] apoptosis (Figure 1E). Moreover, the percent[illegible] of Wilms' tumor cells transfected [illegible]ith miR-61[illegible] mimics increased in the G0/[illegible] but the percentage in the S phased [illegible]eased [illegible]iceably compared with miR-NC [illegible] (Figu[illegible]E). The results indicated that m[illegible] imp[illegible] tumor cell proliferatio[illegible]apa[illegible]ucing cell-cycle arrest at the G[illegible]1 phase[illegible]

MiR-613 Inhi[illegible]ll Migration and Invasio[illegible] vit[illegible]

We nex[illegible] evaluated t[illegible]e of miR-613 in Wilms' t[illegible] cell metastasi[illegible]*tro*. As shown by a w[illegible]d-healing assay, ove[illegible]expressed miR-613 c[illegible] suppr[illegible] Wilms' tumor cell migration co[illegible]d wit[illegible]e negat[illegible] control cells (Figure 2A). [illegible], the e[illegible]ts of miR-613 on cell i[illegible]asion [illegible]red [illegible]answell assay were the [illegible]s the [illegible]esults (Figure 2B). These resu[illegible]demonst[illegible] that miR-613 could inhibit the [illegible]metastasis of Wilms' tumor cells.

[illegible]2 is the Target Gene of miR-613

To better understand the mechanism regard[illegible]y miR-613 participates in these biological proc[illegible]es, we selected FRS2 as a potential downstream target of miR-613 using Target Scan and Star Base database (Figure 3A). Acco[illegible] prediction, miR-613 was transfecte[illegible] a FR[illegible] 3'UTR luciferase reporter gene i[illegible]G401 cells. The results suggested that luci[illegible]activity decreased in Wilms' tumor cells t[illegible]ted with wild-type FRS2 and miR-[illegible] mimic[illegible]pared with cells transfected wi[illegible]utated FRS[illegible] NC (Figure 3B), indic[illegible] that F[illegible]S2 is a t[illegible] gene of miR-613.

Meanwhile, we [illegible]r[illegible]cted t[illegible]RS2 expression level[illegible] W[illegible]umor [illegible] transfected with [illegible]613 mi[illegible]r n[illegible]NC. The results indi[illegible] that FRS2 w[illegible]nregulated in Wilms' [illegible]lls transfecte[illegible]ith miR-613 mimics [illegible]e mR[illegible]nd protein levels compared with miR-NC ce[illegible]ure 3C-D).

F[illegible]more, we als[illegible]ected whether the k[illegible]down of miR-613 could lead to an increase [illegible]e endogenou[illegible]xpression level of FRS2. The [illegible]lts indicated[illegible]t the mRNA and protein le[illegible] of FRS2 we[illegible]levated compared with Inhib[illegible]C cells [illegible]ure 3E-F). These results indicate[illegible]s directly targeted by miR-613.

[illegible]estoration of FRS2 Rescued the Tumor [illegible]ive Role of miR-613

To [illegible]ture identify the interaction of miR-613 and FRS2, we measured the expression level of FRS2 in Wilms' tumor tissues. The results indicated that FRS2 was overexpressed in Wilms' tumor tissues compared with paired normal kidney tissues on the mRNA level (Figure 4A), and the expression level of FRS2 was negatively correlated with the expression level of miR-613 in Wilms' tumor tissues (Figure 4B). Secondly, we explored whether FRS2 is responsible for the functional effects of miR-613 in Wilms' tumor tumorigenesis. We overexpressed FRS2 by transfecting miR-613-overexpressing SK-NEP-1 and G401 cells with pCDNA3.1-FRS2. Also, we downregulated FRS2 expression by transfecting miR-613-overexpressing SK-NEP-1 and G401 cells with siRNA-FRS2 (Figure 4C). FRS2 restoration not only increased the proliferation capacity of miR-613-transfected cells (Figure 4D) and attenuated the cell cycle distribution at the G0/G1 phase (Figure 4E), but it also increased the cell migration and invasion capacities partially compared with miR-613-NC cells (Figure 4F-G). Meanwhile, knockdown of FRS2 phenocopied miR-613 overexpression (Figure 4C and G). The results implied that miR-613 suppressed Wilms' tumor tumorigenesis by regulating FRS2.

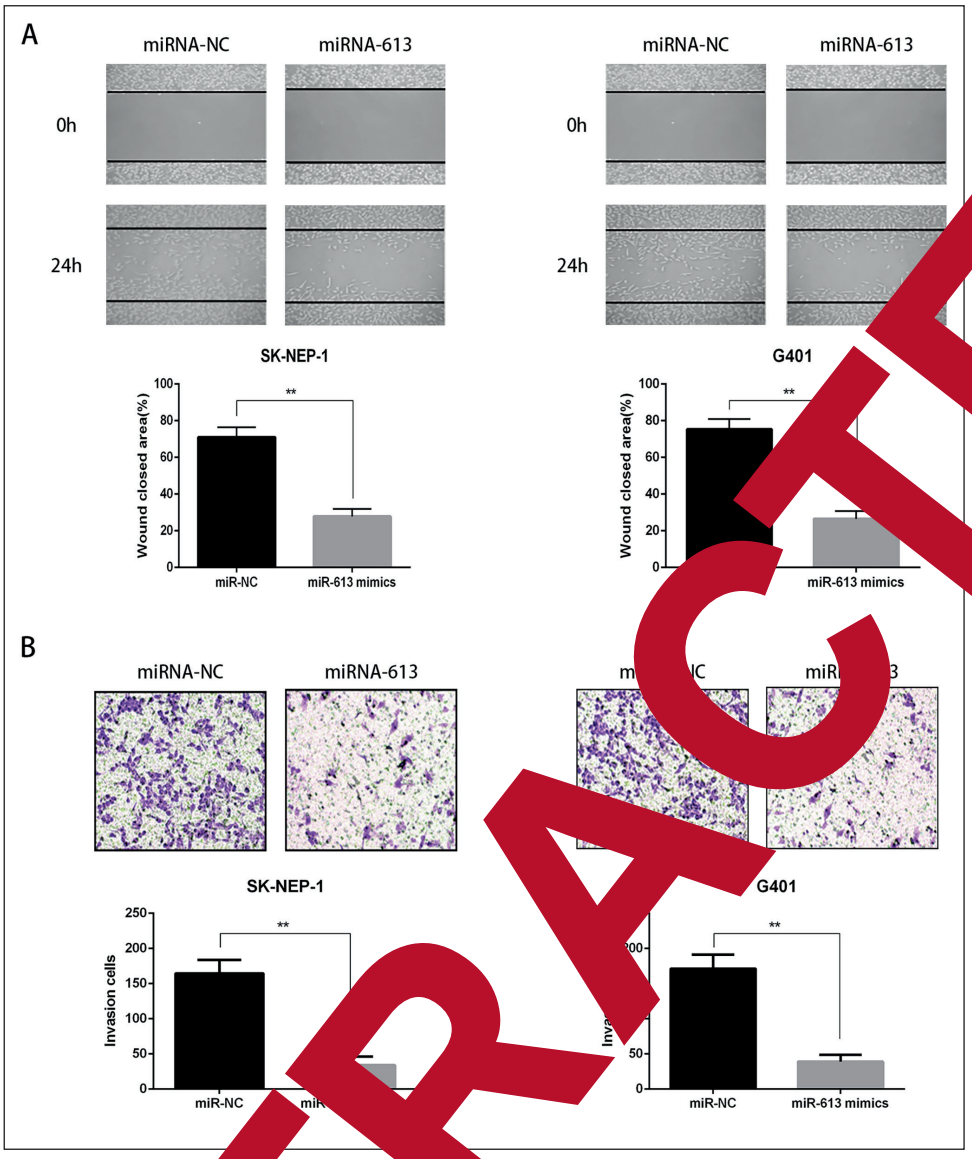

Figure 2. MiR-613 inhibited cell and inva A wo caling ass was ormed to assell migration capa SK-NEP-1 and G4 trans- ected wi mimics and mi A t ell assay pe ed to assess ll invas apac- of SK -1 and 01 ce ansfected 13 mimics a NC. Data are prese d as the mean ± SD of three independent experiments. $^{**}p < 0.01$.

Discussi

Th thoge of Wilms' tumor is not clear at pre The h nesis n ly includes a "two hit mode nd "n ogenic rest theory"[16,17], but any hyp ses alone has its limitaexpl nogenesis of the tumor. In rece ears, due he rapid development of molecu iology, many Researches have determined th nt progression of Wilms' tumor be attributed to abnormal activation of mul- signaling pathways, such as Stat3[18], WT1[19], and TP53 signaling pathways[21], which provide new direction for the treatment of Wilms' tumor pathogenesis. More and more studies have suggested that miRNAs play a crucial role in carcinogenesis and the cancer progression of various types of tumors. For example, Karimi Dermani et al[22] found that resveratrol could inhibit apoptosis, inhibit invasion, and switch from an EMT to MET phenotype through the upregulation of miR-200c in colorectal cancer. Shen et al[23] demonstrated that miR-660-5p functions as an oncogene in human breast cancer via targeting TFCP2 and may provide a promising therapeutic strategy for the treatment of breast cancer. Tian et al[24] revealed that miR-509-5p inhibited the cell proliferation and metastasis of prostate cancer by targeting MDM2.

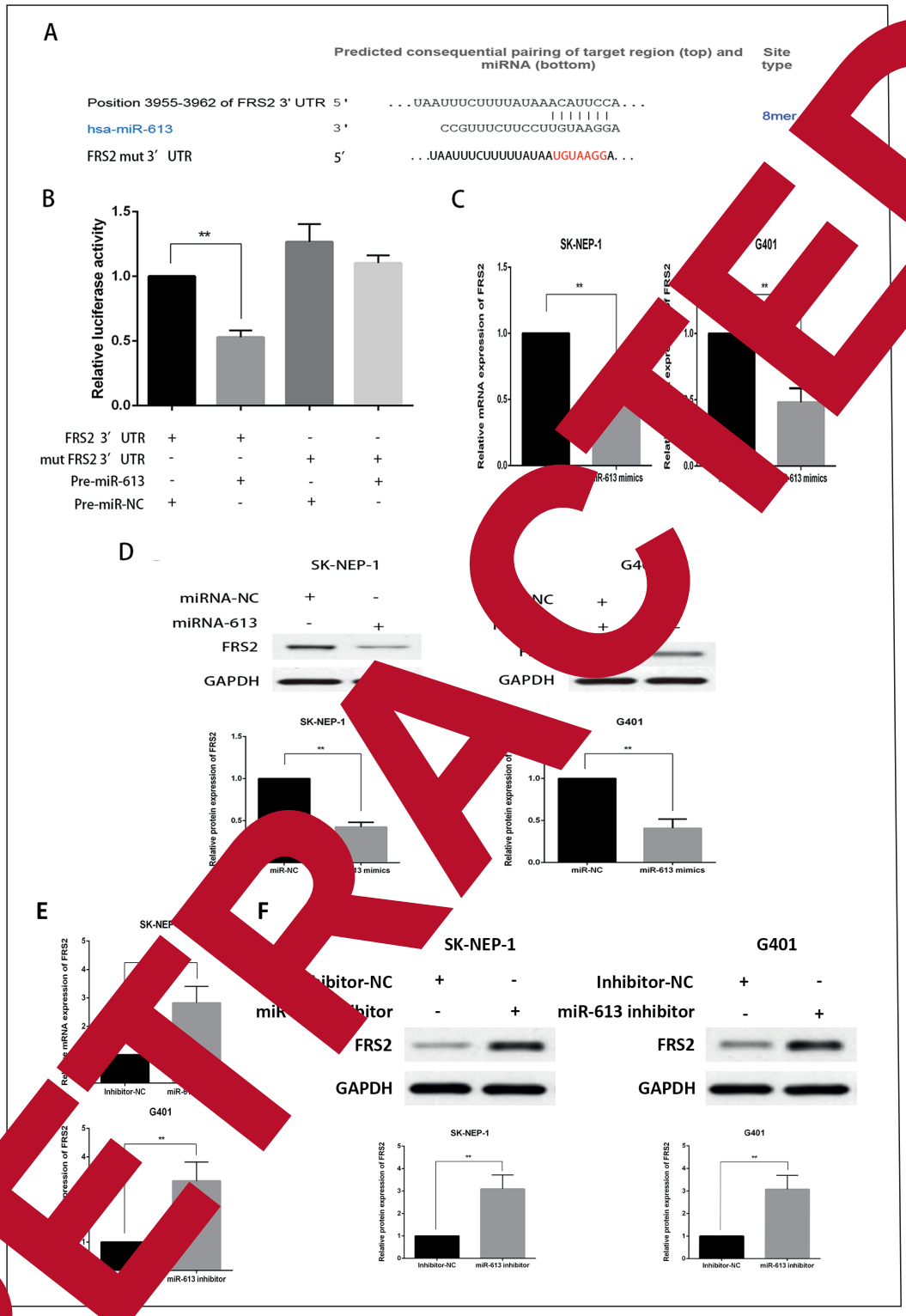

Figu FRS2 is the target gene of miR-613. **A**, FRS2 was selected as the potential downstream target of miR-613 using bio sis; **B**, Luciferase activities of G401 cells transfected with the wild-type or mutated FRS2 3′UTR togeth- miR-613 mimics or miR-NC; **C**, FRS2 mRNA expression level of SK-NEP-1 and G401 cells transfected with miR-613 ics or miR-NC; **D**, FRS2 protein expression level in SK-NEP-1 and G401 cells transfected with miR-613 mimics or miR- ta are presented as the mean ± SD of three independent experiments. **E**, FRS2 mRNA expression level in SK-NEP-1 a cells transfected with miR-613 inhibitor or Inhibitor-NC; **F**, FRS2 protein expression level in SK-NEP-1 and G401 cells t fected with miR-613 inhibitor or Inhibitor-NC. $^{**}p < 0.01$.

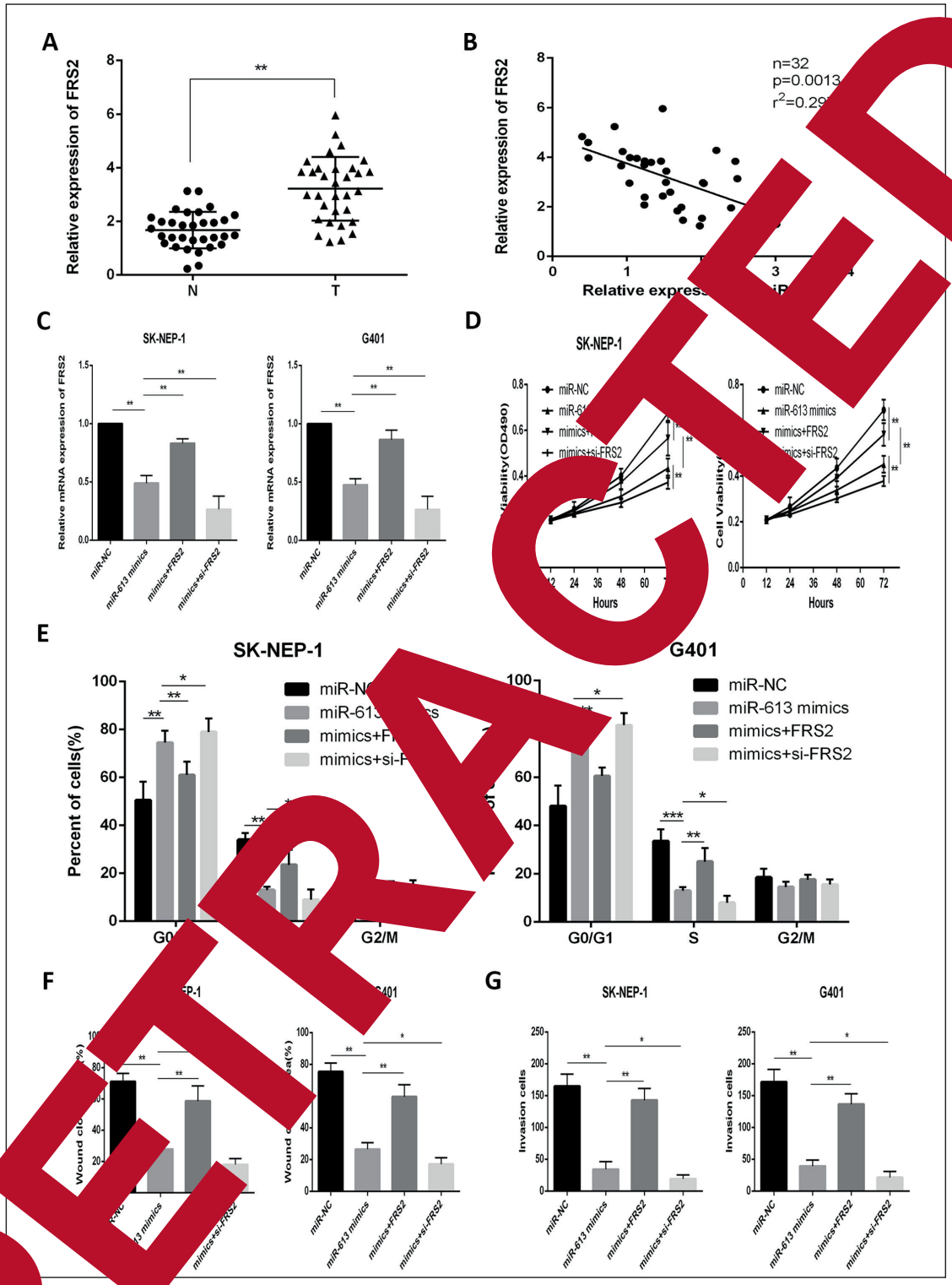

Figu Restoration of FRS2 rescued the tumor suppressive role of miR-613. **A**, FRS2 expression level in Wilms' tumor tis nal matched control kidney tissues (N), n=32; **B**, Correlation between miR-613 and FRS2 expression in tumor tissues (n=32); **C**, Transfection efficiency in SK-NEP-1 and G401 cells transfected with miR-613 negative control (NC), mimics, and/or pCDNA3.1-FRS2or siRNA-FRS2; **D**, The effect of ectopic expression of FRS2 on cell proliferation; lysis of the effect of ectopic expression of FRS2 on cell cycle; **F**, The effect of ectopic expression of FRS2 on cell mi- The effect of ectopic expression of FRS2 on cell invasion. Data are presented as the mean ± SD of three independent riments. $*p < 0.05$, $**p < 0.01$, $***p < 0.001$.

Du et al[25] reported that miR-543 promotes the cell growth and metastasis of prostate cancer via targeting RKIP. Several reports have investigated the role of miRNAs in Wilms' tumor tumorigenesis. Guo et al[26] found that miR-206 could promote podocyte injury in adriamycin-induced nephropathy via targeting FRS2. He et al[15] demonstrated that transcription factors, miRNAs, target genes and the host gene-differentially expressed network could accurately reveal the pathogenesis of Wilms' tumor. To date, there has been no systematic study of the relationship between miR-613 and Wilms' tumor tumorigenesis. In this investigation, we demonstrated that miR-613 was downregulated in Wilms' tumor tissues compared with adjacent normal tissues, implying that miR-613 plays a potential and vital role in the progression and development of Wilms' tumor. In addition, overexpression of miR-613 attenuated Wilms' tumor cell viability, proliferation, invasion and migration capacity, as well as induced cell cycle arrest at the G0/G1 phase. Taken together, these findings suggest that miR-613 exerts a suppressive effect on the cell proliferation and metastasis of Wilms' tumor. To further identify the underlying mechan of how miR-613 inhibits Wilms' tumor cell genesis and metastasis, we predicted and s ed FRS2 as a novel target of miR-613 by bioinfo tics analysis. FRS2 (Fibroblast Growth Factor 2 involved in the tumorigenesis of certain types malignancies, including breast and prostate cancer[28]. FRS2 might r te tu genesis primarily via mediating m nic FG naling in prostate cancer and m ve a biomarker for hormo re tive breast cancer patients. FR an also egulated by miRNAs in tumor esis, such as 6 in gastric cancer[29]. In we revealed t FRS2 is directly tar d by 613, and the miR-613 expression l er is inverse elated with FRS2 in Wilms or tissues. Mor the restoration of FRS ld rescue the tumor suppressive role of miR- n Wil tumor cell growth and metasta hile t ockdo of FRS2 phenocopied miR- pressio

nclusions

rated that miR-613 has a tu- suppressive effect on Wilms' tumor pro- sion and metastasis via targeting FRS2 *in* ur findings may help to further elucidate the ecular mechanisms underlying Wilms' tumor progression and indicate miR-613 as an innovative target for diagnosis and t Wilms' tumor.

Conflict of Interest

The Authors declare that they ha conflict o

Re nces

1) Martinez CH, Dave Wilms' . Adv Exp Med Bi 10; c -209.
2) Zhang R, Y JY, Sun F H J, Shi YJ, Li G. C ison of mini dal disease (MRD) by WT1 qua ation between child ac loid leukemia and acute lymphob tic leuke r Rev Med Pharmacol Sci 2015; 19: 2679-26
3) SJ, Chen ZH, Z H, Zhou H, Li LS, Liu . Evaluation of podocyte lesion in patients with diabetic nephropathy: Wilms' tumor-1 protein used as a p cyte marker. Diabetes Res Clin Pract 2010; 8 7-175.
4) ngstrom W, nerus M. The expression of the lin-like th factor II, JIP-1 and WT1 genes roblastoma. Anticancer Res 2009; 29: 003.
5) Cardoso LC, De Souza KR, De O RA, Andrade RC, itto AJ, De Lima MA, Dos SA, De Faria PS, Ferman nez HN, Vargas FR. WT1, WTX and CTNNB1 tion analysis in 43 patients with sporadic Wilms' tumor. Oncol Rep 2013; 29: 315-320.
6) Theerakitthanakul K, Khrueathong J, Kruatong J, Graidist P, Raungrut P, Kayasut K, Sangkhathat S. Senescence Process in Primary Wilms' Tumor Cell Culture Induced by p53 Independent p21 Expression. J Cancer 2016; 7: 1867-1876.
7) Adlakha YK, Seth P. The expanding horizon of MicroRNAs in cellular reprogramming. Prog Neurobiol 2017; 148: 21-39.
8) Koshizuka K, Hanazawa T, Fukumoto I, Kikkawa N, Okamoto Y, Seki N. The microRNA signatures: Aberrantly expressed microRNAs in head and neck squamous cell carcinoma. J Hum Genet 2017; 62: 3-13.
9) Wang X, Chen L, Jin H, Wang S, Zhang Y, Tang X, Tang G. Screening miRNAs for early diagnosis of colorectal cancer by small RNA deep sequencing and evaluation in a Chinese patient population. Onco Targets Ther 2016; 9: 1159-1166.
10) Zhuang Y, Peng H, Mastej V, Chen W. MicroRNA regulation of endothelial junction proteins and clinical consequence. Mediators Inflamm 2016; 2016: 5078627.
11) Ren W, Li C, Duan W, Du S, Yang F, Zhou J, Xing J. MicroRNA-613 represses prostate cancer cell proliferation and invasion through targeting Frizzled7. Biochem Biophys Res Commun 2016; 469: 633-638.
12) Wu J, Yuan P, Mao Q, Lu P, Xie T, Yang H, Wang C. MiR-613 inhibits proliferation and invasion of breast cancer cell via VEGFA. Biochem Biophys Res Commun 2016; 478: 274-278.

13) Li X, Sun X, Wu J, Li Z. MicroRNA-613 suppresses proliferation, migration and invasion of osteosarcoma by targeting c-MET. Am J Cancer RES 2016; 6: 2869-2879.
14) Li B, Xie Z, Li Z, Chen S, Li B. MicroRNA-613 targets FMNL2 and suppresses progression of colorectal cancer. Am J Transl Res 2016; 8: 5475-5484.
15) He J, Guo X, Sun L, Wang K, Yao H. Networks analysis of genes and microRNAs in human Wilms' tumors. Oncol Lett 2016; 12: 3579-3585.
16) Md ZR, Murch A, Charles A. Pathology, genetics and cytogenetics of Wilms' tumour. Pathology 2011; 43: 302-312.
17) Yin M, Cai J, Thorner PS. Congenital renal tumor: Metanephric adenoma, nephrogenic rest, or malignancy? Pediatr Dev Pathol 2015; 18: 245-250.
18) Wang J, Zhang N, Qu H, You G, Yuan J, Chen C, Li W, Pan F. Inhibitory effect of STAT3 gene combined with CDDP on growth of human Wilms tumour SK-NEP-1 cells. Biosci Rep 2016; 36:
19) Singh A, Mandal A, Guru V, Seth R. Acute lymphoblastic leukemia mimicking Wilms tumor at presentation. Gulf J Oncolog 2016; 1: 76-79.
20) Zhang YY, Wang QM, Niu HL, Liu X, Zhang QL. The general expression analysis of WTX gene in normal and cancer tissues. Pathol Oncol Res 2017; 23: 439-446.
21) Ooms AH, Gadd S, Gerhard DS, Smith MA, Guidry AJ, Meerzaman D, Chen QR, Hsu CH, Yan C, Nguyen C, Hu Y, Ma Y, Zong Z, Mungall AJ, Mo[illegible] Marra MA, Huff V, Dome JS, Chi YY, Tian[illegible] JI, Mullighan CG, Ma J, Wheeler DA, Hamp[illegible]DA, Walz AL, van den Heuvel-Eibrink MM, de Krij[illegible], Ross N, Gastier-Foster JM, Perlman EJ. Signific[illegible] of TP53 mutation in wilms tumors with diff[illegible] anaplasia: A report from the chil[illegible]'s oncolog[illegible] group. Clin Cancer Res 201[illegible]-5591.
22) Karimi Dermani F, Saidijam M, Amini R, Mahdavinezhad A, Heydari K, Najafi R. Resveratrol i[illegible] liferation, invasion, and epithelial[illegible] transition by increasing miR-200[illegible]pression HCT-116 colorectal cancer cell[illegible]Cell Biochem 2017; 118: 1547-1555.
23) Shen Y, Ye YF, Ruan LW, Bao L, [illegible]Y, Zhou Y. Inhibition of miR-660-5p[illegible]xpressio[illegible]esses tumor development a[illegible]etastasis[illegible] breast cancer. Genet[illegible]Res 2017; 16:
24) Tian XM, Luo YZ, He[illegible]J, Ma Z[illegible]An Y. Inhib[illegible] of invasion and m[illegible]on of p[illegible]te cancer cells by miRNA-509-[illegible]tar[illegible]g MDM[illegible]Genet Mol Res 201[illegible]6:
25) Du Y, Liu X[illegible]u HC, [illegible]Nin[illegible]Xiao CC. MiR-543 [illegible]otes proliferat[illegible]melial-Mesenchym[illegible]ition in prostate[illegible]via targeting RKIP[illegible]Biochem 2017; [illegible]: 1135-1146.
26) Guo[illegible]Guo[illegible]D. MicroRNA-206 and its down-regulation [illegible]s'Tumor-1 dictate podocyte health in adria[illegible]induced nephropathy. [illegible]il 2016; 38: 989[illegible].
[illegible]hong X, Xie G, Zhang Z, Wang Z, Wang Y, Wang Y, Qiu Y, Li L, Bu[illegible]Li J, Zheng H. MiR-4653-3p and its target ge[illegible]RS2 are prognostic biomarkers for hormone [illegible]ptor positive breast cancer pa[illegible]nts receivi[illegible]amoxifen as adjuvant endocrine [illegible]y. O[illegible]rget 2016; 7: 61166-61182.
28) L[illegible]en G, Fu X, Zeng X, Wang C, Huang Y, An L, Wan X, Navone N, Wu CL, McKeehan WL, Zhang Z, Zhong W, Wang F. Hyperactivated FRS2alpha-me[illegible]d signaling in prostate cancer cells promotes tu[illegible]giogenesis and predicts poor clinical outcome of patients. Oncogene 2016; 35: 1750-1759.
29) Ren J, Huang HJ, Gong Y, Yue S, Tang LM, Cheng SY. MicroRNA-206 suppresses gastric cancer cell growth and metastasis. Cell Biosci 2014; 4: 26.